

Stability Enhancement of Integrated ZnO/Zn₃As₂/SrTiO₃ Photocatalyst for Photocatalytic Over-all water Splitting

Zhiquan Yin^{a,b}, Wenlong Zhen^a, Xiaofeng Ning^a, Zhengzhi Han^a, Gongxuan Lu^{*a}

^a State Key Laboratory of Low Carbon Catalysis and Carbon Dioxide Utilization, Lanzhou Institute of Chemical Physics, Chinese Academy of Sciences, Lanzhou 730000, China

^b University of Chinese Academy of Sciences, Beijing 100049, China

1. Experimental section

1.1 Preparation of SrTiO₃ sample

According to literature reports, the SrTiO₃ photocatalyst was prepared using the high-temperature molten salt method.¹ Briefly, 14.53 g SrCl₂·6H₂O, 41 mg Al(NO₃)₃·9H₂O, and 1 g SrTiO₃ powder were thoroughly ground. The mixture was heated to 1150 °C for 10 hours at a rate of 10 °C·min⁻¹ in a corundum crucible under an air atmosphere. After cooling to room temperature, the product was rinsed with deionized water and filtrated until the filtrate was neutral and dry at 60 °C.

Co-catalysts were loaded via an impregnation-calcination method. In a typical preparation, 500 mg of molten salt method treated SrTiO₃ powder, 1.0 mg RhCl₃, 3.8 mg Cr(NO₃)₃·9H₂O, and 2.5 mg Co(NO₃)₃·6H₂O were dispersed into 5 mL of deionized water under constant stirring and ultrasonic dispersion for 5 min, respectively. The mixing suspension was dried at 80 °C under stirring, and the dried sample was ground evenly and calcined at 350 °C for 1 hour at a heating rate of 10 °C·min⁻¹ in an air atmosphere. After cooling to room temperature, the obtained powder of SrTiO₃ was collected.

1.2 Photoelectrochemical performance

Photoelectrochemical data were acquired on an electrochemical analyzer (CHI660E). Photoelectrochemical experiments were carried out in a three-electrode cell with a quartz window (diameter = 1.2 cm) facing the working electrode. The samples were dropped on the surface of the cleaned indium tin oxide glass (ITO glass)

as a working electrode, and the contact area between the sample and electrolyte was controlled to be about 1 cm². A platinum sheet and a saturated calomel electrode (SCE) were used as the counter and reference electrodes, respectively. The photocurrent-time curve (IT) of the cathode was acquired without bias. The linear sweep voltammetry curve (LSV) had a sweep rate of 0.5 mV·s⁻¹. A 300 W xenon lamp with a 420 nm cut-off filter served as the excitation source, and the electrolyte was 0.1M Na₂SO₄ solution.

1.3 Characterization of the catalysts

The crystallographic information of the catalyst was recorded using a Rigaku B/Max-RB X-ray powder diffractometer (XRD) equipped with a nickel-gate CuK α target at a sweep rate of 0.01°·s⁻¹ over a 10-80° diffraction range. X-ray photoelectron spectroscopy (XPS) of the sample was performed using VG Scientific ESCALAB210-XPS photoelectron spectrometer using an Al K α X-ray source. The Tecnai-G2-F30 field emission transmission electron microscope (TEM) was used to capture TEM and high-resolution TEM (HR-TEM) images of the sample at an acceleration voltage of 300 kV. The photoluminescence spectra (PL) and time-resolved PL (TR-PL) (excitation wavelength is 970 nm) of the samples were obtained by Hitachi F-4500 photoluminescence spectrometer. The UV-vis-NIR diffuse reflectance spectrum (UV-vis-NIR DRS) of the sample was collected by the PerkinElmer Lambda 950 UV/vis/NIR spectrometer with BaSO₄ powder as the internal standard. The concentration of arsenic (As³⁺) ions in the aqueous solution of the reaction system was determined using the contrAA700 atomic absorption spectrometer (AAS).

1.4 Photocatalytic splitting D₂O and H₂¹⁸O isotope-labeled experiments

The isotope tracer experiments were performed in a mini-reactor to investigate the photocatalytic splitting of D₂O and H₂¹⁸O. Typically, 10 mg of catalyst was dispersed in 10 mL D₂O or 2 mL H₂¹⁸O in the sealed quartz flask. After ultrasonic treatment for 30 min, the sealed suspension system was bubbled with argon flow for 30 min to remove air from the reactor. After visible light irradiation for 6 hours, the mixed gas was analyzed by MS (TILON LC-D200M mass spectrometer, equipped with a high vacuum sampling valve, quartz glass capillary tube, and capillary temperature

maintained at 120 °C).

1.5 The reverse reaction experiments of H₂ and O₂

The H₂-O₂ recombination experiments were conducted in a sealed reactor, the same as the reactor used in photocatalytic experiments. The specific experimental process was described as follows. In the reactor, 20 mg of photocatalyst was ultrasonically dispersed in 100 mL de-ionized water. To exclude air as much as possible, the reactor was purged with high-purity Ar. After that, H₂ (1.2 mL) and O₂ (0.6 mL) were injected into the reactor to imitate the H₂-O₂ reverse reaction under dark conditions.

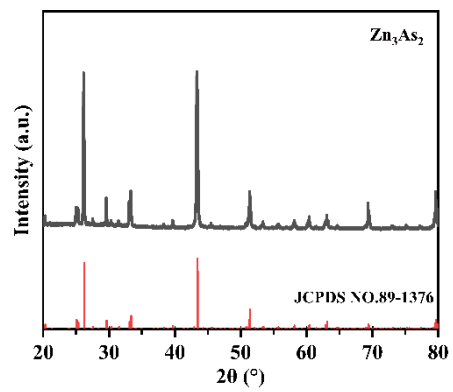


Figure S1 XRD patterns of Zn₃As₂ and corresponding JCPDS card.

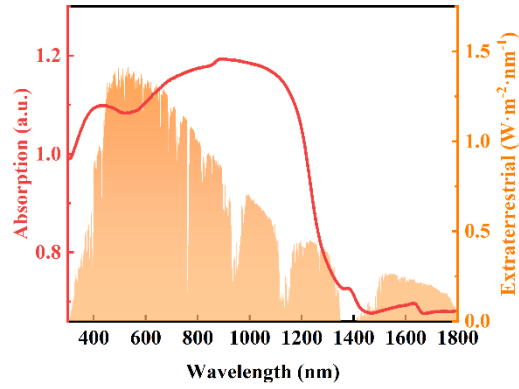


Figure S2 UV-vis-NIR DRS of Zn₃As₂.

Figure S2 shows the UV-vis-NIR DRS of Zn₃As₂, revealing a distinct absorption edge at approximately 1250 nm, which corresponds to a solar spectral coverage of ~85% in the solar spectrum. The broad spectral response spanning the ultraviolet to near-infrared regions, coupled with an exceptionally high absorption coefficient, establishes Zn₃As₂ as a promising light-harvesting candidate for next-generation optoelectronic devices.

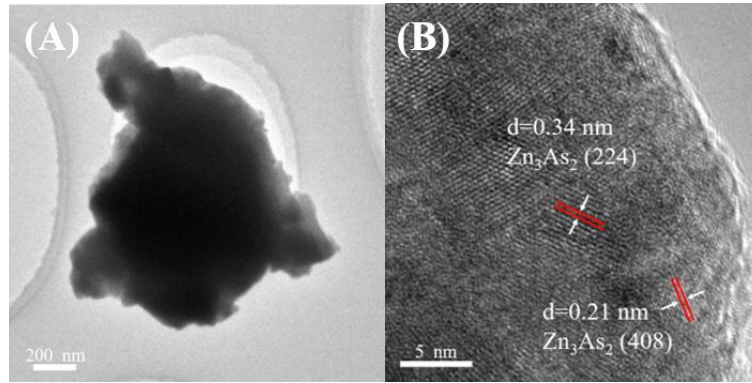


Figure S3 (A) TEM and (B) HR-TEM images of Zn_3As_2 .

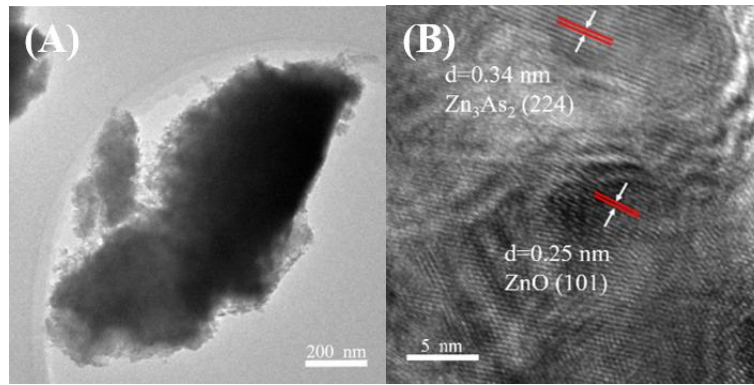


Figure S4 (A) TEM and (B) HR-TEM images of ZnO/ Zn_3As_2 .

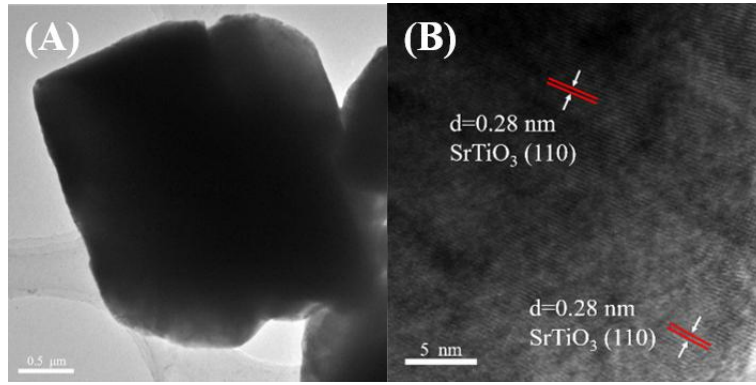


Figure S5 (A) TEM and (B) HR-TEM images of SrTiO₃.

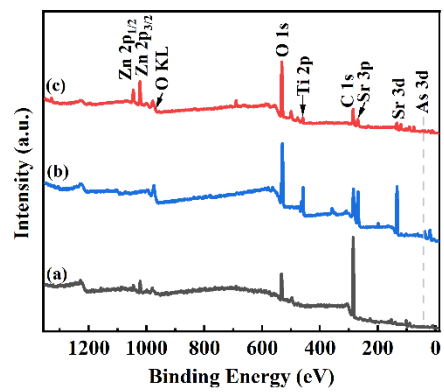


Figure S6 XPS survey spectra of (a) ZnO/Zn₃As₂, (b) SrTiO₃, and (c) ZnO/Zn₃As₂/SrTiO₃.

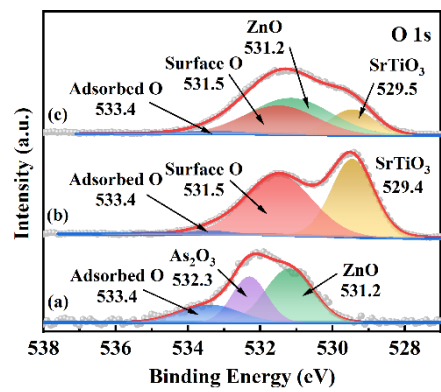


Figure S7 O 1s spectra of (a) ZnO/Zn₃As₂, (b) SrTiO₃, and (c) ZnO/Zn₃As₂/SrTiO₃.

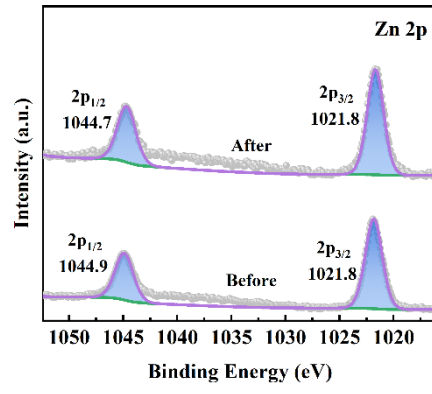


Figure S8 Zn 2p spectra of Zn₃As₂ before and after reaction.

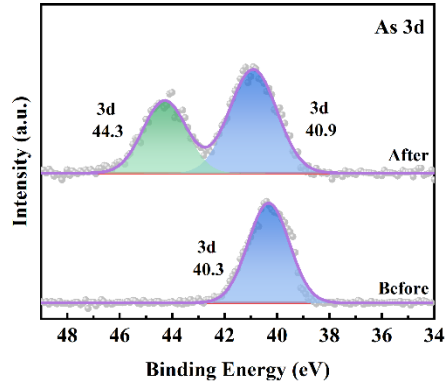


Figure S9 As 3d spectra of Zn₃As₂ before and after reaction.

Figure S9 shows the As 3d XPS spectra of Zn₃As₂ before and after the photocatalytic reaction. Before the photocatalytic reaction, the characteristic peak of As 3d was located at 40.3 eV, corresponding to As³⁻ in Zn₃As₂. After 3 hours of photocatalytic reaction, the As 3d spectrum can be deconvoluted into two peaks at 40.9 eV and 44.3 eV, respectively, assigned to Zn₃As₂ and As₂O₃. However, the conductivity of As₂O₃ is very low, and the transport of photo-excited charge carriers is significantly hindered by the abundant As₂O₃ on the surface of Zn₃As₂.² Thus, during the photocatalytic water splitting process of Zn₃As₂, the formation of As₂O₃ via surface oxidation drastically suppresses the hydrogen evolution activity of Zn₃As₂.

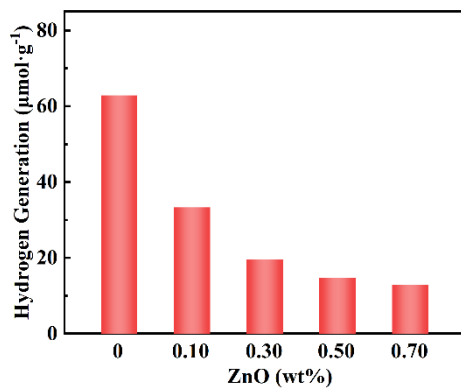


Figure S10 The photocatalytic hydrogen production activity of ZnO/Zn₃As₂ photocatalysts with different ZnO content in 3 h under visible light irradiation.

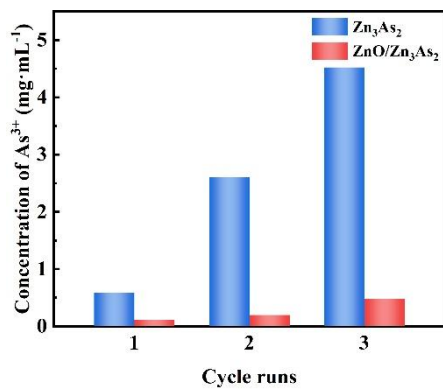


Figure S11 The As^{3+} ion concentration in reaction solution of Zn_3As_2 and $\text{ZnO}/\text{Zn}_3\text{As}_2$ composite with visible light irradiation time.

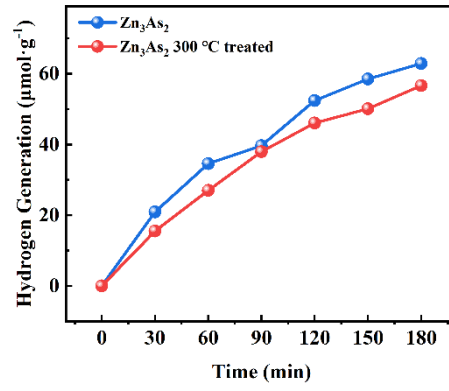


Figure S12 The photocatalytic hydrogen production activity of Zn₃As₂ photocatalysts.

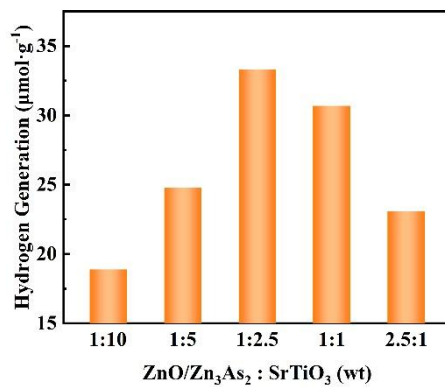


Figure S13 The photocatalytic hydrogen production activity of ZnO/Zn₃As₂/SrTiO₃ photocatalysts with different ZnO/Zn₃As₂ content in 3 h (the hydrogen production content calculation with ZnO/Zn₃As₂).

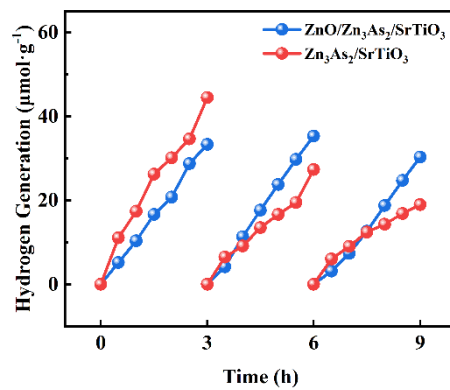


Figure S14 The photocatalytic hydrogen production activity of Zn₃As₂/SrTiO₃ (1:2.5 mass rate) and ZnO/Zn₃As₂/SrTiO₃ photocatalysts in 3 h (the hydrogen production content calculation with Zn₃As₂).

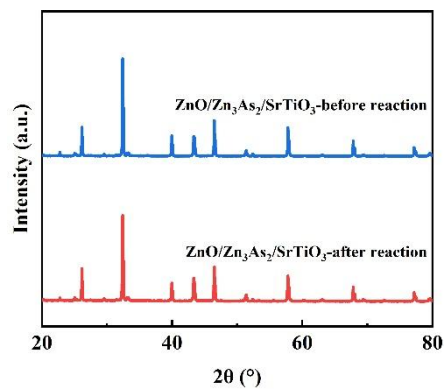


Figure S15 XRD patterns of ZnO/Zn₃As₂/SrTiO₃ photocatalyst.

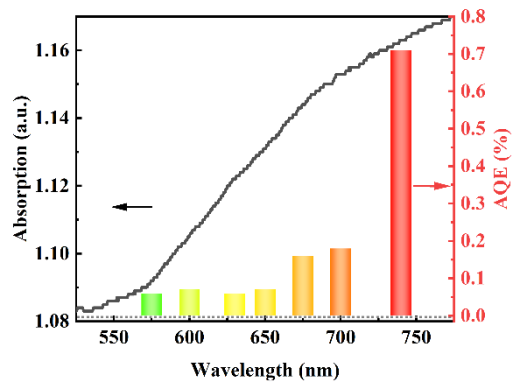


Figure S16 The apparent quantum yield on ZnO/Zn₃As₂/SrTiO₃ photocatalyst.

Table S1 The apparent quantum efficiency (AQEs) of reported samples for long-wavelength visible light (>600 nm) for H₂ evolution reaction by photocatalytic overall water splitting.

NO.	Photocatalyst	Solution	AQE	Ref.
1	ZnO/Zn ₃ As ₂ /SrTiO ₃	H ₂ O	0.71% at 740 nm	This work
2	α -Fe ₂ O ₃ /RP	H ₂ O	0.002% at 700 nm	3
3	sp ² c-Py-BT COF	H ₂ O	0.22% at 650 nm	4
4	Cu ₂ ZnSnS ₄ /CdS/TiO ₂ /Pt	H ₂ O	0.03% at 675 nm	5
5	Y ₂ Ti ₂ O ₅ S ₂	H ₂ O	0.05% at 600 nm	6
6	Pt/Ni(OH) ₂ -C ₃ N ₄	H ₂ O	0.05% at 600 nm	7
7	BiFeO ₃ /COF	H ₂ O	0.32% at 650 nm	8
8	ZnSe-Znv	H ₂ O	0.15% at 600 nm	9
9	boron phosphide @ g-C ₃ N ₄	H ₂ O	0.005% at 730 nm	10

References:

- 1 T. Takata, J. Jiang, Y. Sakata, M. Nakabayashi, N. Shibata, V. Nandal, K. Seki, T. Hisatomi and K. Domen, *Nature*, 2020, **581**, 411-414.
- 2 V. Suryanarayana, A. V. Sekhar, A. Bafti, L. Pavić, A. S. S. Reddy, G. N. K. Reddy, N. Venkatramaiah, V. R. Kumar and N. Veeraiah, *Journal of Non-Crystalline Solids*, 2023, **610**, 122299.
- 3 S. Jiang, X. Jia, J. Cao, H. Lin, F. Li, Y. Sun and S. Chen, *Inorganic Chemistry* 2022, **61**, 18201-18212.
- 4 J. Cheng, Y. Wu, W. Zhang, J. Zhang, L. Wang, M. Zhou, F. Fan, X. Wu and H. Xu, *Advanced Materials* 2024, **36**, 2305313.
- 5 X. Zhang, G. Lu, Y. Wu, J. Dong and C. Wang, *Catalysis Science & Technology* 2021, **11**, 5505-5517.
- 6 Q. Wang, M. Nakabayashi, T. Hisatomi, S. Sun, S. Akiyama, Z. Wang, Z. Pan, X. Xiao, T. Watanabe, T. Yamada, N. Shibata, T. Takata and K. Domen, *Nature Materials* 2019, **18**, 827-832.
- 7 S. Sun, Y. Zhang, G. Shen, Y. Wang, X. Liu, Z. Duan, L. Pan, X. Zhang and J. Zou, *Applied Catalysis B: Environmental* 2019, **243**, 253-261.
- 8 M. Xu, M. Lu, G. Qin, X. Wu, T. Yu, L. Zhang, K. Li, X. Cheng and Y. Lan, *Angewandte Chemie International Edition* 2022, **61**, e202210700.
- 9 X. Wang, X. Sui, M. Wang, Z. Zheng, H. Yuan, S. Yang, H. G. Yang, Y. Peng and Y. Hou, *Applied Catalysis B: Environment and Energy* 2025, **365**, 124937.
- 10 B. Tian, Y. Wu, G. Lu, *Applied Catalysis B: Environmental* 2021, **280**, 119410.